J. Fluid Mech. (1991), *vol.* 233, *pp.* 519–537
Printed in Great Britain

On the shape of small sessile and pendant drops by singular perturbation techniques

By S. B. G. O'BRIEN†
Philips Research Laboratories, P.O. Box 80000, 5600 JA Eindhoven, The Netherlands

(Received 8 December 1990)

The problem of obtaining asymptotic expressions describing the shape of small sessile and pendant drops is revisited. Both cases display boundary-layer behaviour and the method of matched asymptotic expansions is used to obtain solutions. These give good agreement when compared with numerical results. The sessile solutions are relatively straightforward, while the pendant drop displays a behaviour which is both rich and interesting.

1. Introduction

The shape of liquid drops has long been a source of fascination to engineers, physicists and mathematicians. The physics of curved fluid–liquid interfaces has long been understood, the fundamental equation (equation (1)), which postulates a jump in the pressure across any *curved* interface, having originally been derived by Laplace. Mathematically the equation has remained of interest owing to its nonlinearity: even in the axisymmetric case, when (1) reduces to an ordinary differential equation, no general solution is possible. It has thus proved necessary to resort to numerical solutions, the first of these being the hand-calculated tables of Bashforth & Adams (1883) who computed the shape of liquid drops as a function of surface tension and drop size. These results have been significantly improved upon in recent times with the advent of digital computers. Of considerable interest is the work of Padday (1971) who combines numerical solutions with a qualitative and quantitative account of the different axisymmetric profiles which can arise. The most comprehensive computations performed to date have been those of Hartland & Hartley (1976) who used a fourth-order Runge–Kutta method claiming accuracy to within one part in a million. Furthermore they did not restrict their calculations to drop shapes: also included were external menisci shapes as for example occur when an axisymmetric object is placed in an infinite sea of liquid. Their work includes extensive tables of numerical results. At this stage one might wonder what the particular fascination is for these solutions. From an aesthetic point of view it is a challenge to be able to describe the shape of a liquid drop as a function of the relevant physical parameters: all the more as these solutions can be readily compared with experimental values and the soundness of the physical theory checked. Conversely it is also possible to use a knowledge of drop shape to indirectly measure surface tension or contact angle as illustrated by Padday & Pitt (1972), Shanahan (1982) and O'Brien & van den Brule (1991). So a knowledge of drop shape is also of practical use. The aim of the present paper is to reconsider the problem of deriving an analytic solution for the shape of small sessile and pendant drops. A sessile drop may be defined as one in equilibrium *resting* on a flat horizontal surface (figure 1) while a

† Current address: Mathematical Institute, 24–29 St Giles', Oxford OX1 3LB, UK.

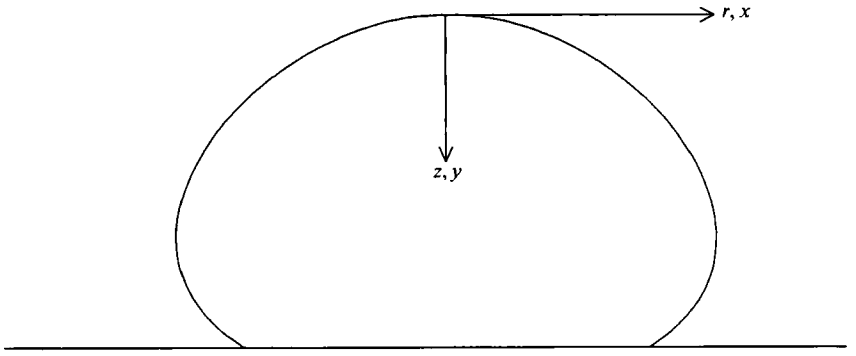

FIGURE 1. Physical and dimensionless coordinate system for a sessile drop.

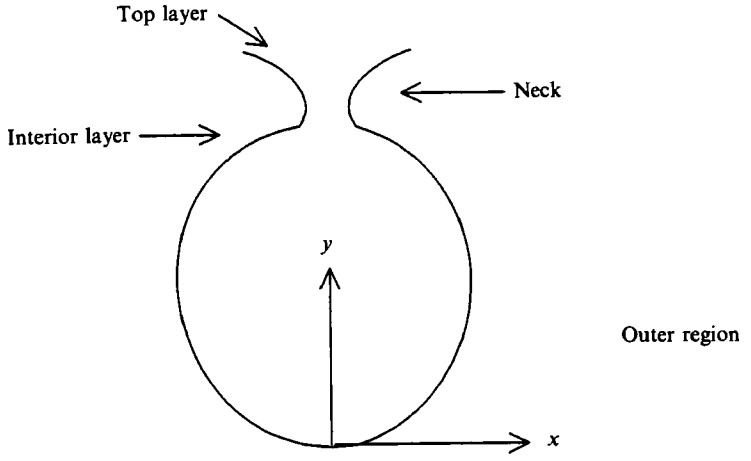

FIGURE 2. Schematic drawing of pendant drop showing outer, neck regions (not to scale).

pendant drop is one which *hangs* from a horizontal ceiling (figure 2). Though the equations describing the shape of both drops are similar, the body forces have opposing effects tending in the former case to flatten the drop and in the latter to draw out or elongate the shape. Note in particular the neck region in the pendant drop which is mathematically extremely interesting as we shall see.

These problems have already been considered by Chesters (1977) but in a less than rigorous fashion, a number of *ad hoc* assumptions being made in order to simplify the equations. In contrast, we shall show, by means of an alternative formulation of the problem, that both the sessile and pendant problems can be solved by a parameter perturbation, the small parameter being the dimensionless drop radius. One of the weaknesses of Chesters' approach was that his perturbation quantity was a variable quantity, which left some doubt as to the accuracy of the solutions even though they compared favourably with numerical solutions. Furthermore, he obtained different solutions for different portions of the drop and matching of these component solutions had to be performed in an *ad hoc* fashion. Extension to higher-order solutions was thus not possible. As we shall see, his difficulties arise from his adoption of the traditional formulation of the problem in terms of the unknown radius of curvature at the apex of a drop. It is simpler to use the maximum radius of the drop as a lengthscale as suggested by Padday (1971) and used for example by Rienstra (1990) and Kuiken (1991) and the present paper investigates an alternative

formulation of the traditional second-order equation (2) as a pair of coupled first-order equations, using the inclination as a parameter. Our solutions will be shown to be an improvement on Chesters' in all cases: some differences arise in the asymptotic expressions. Furthermore higher-order solutions in the sessile case can be obtained by standard techniques. Mathematically, the solutions are also of some interest. The sessile perturbation solutions have already been considered in O'Brien & van den Brule (1991) and are improved upon here where they will be shown to be regular everywhere except in a small boundary-layer region where the inclination approaches π rad. Singular perturbation techniques are necessary to describe the shape in this region. In practice this boundary layer is only of importance in the case where the contact angle approaches π rad, which can occur, for example, in the case of water drops on a dirty surface. The pendant solutions are the real aim of this paper and are somewhat more complicated: a glance at figure 2 suggests that the solution in the neck region will be qualitatively somewhat different from that in the lower nearly spherical region. Singular perturbation techniques are again necessary and in fact it turns out that the upper region can be described in boundary-layer terms but another transition or interior boundary layer, analogous to the boundary layer of the sessile drop, occurs between the lower and neck regions and is necessary for the matching of these regions. Note also the occurrence of a point of inflexion: in the pendant case the boundary-layer behaviour is more fundamental since the inclination will always approach π rad as this point is approached. In the course of our analysis we will be able to obtain an expression for the position at which inflexion occurs and indeed show that a sequence of such points can exist, each one corresponding to the beginning of a new drop joined to its adjacent neighbours by a thin neck region.

The aim of the present paper is thus to reformulate the drop problem into a system which can be more readily solved by means of singular perturbation techniques. This method yields accurate results when compared to numerical solutions provided the drop is small enough in a sense to be discussed more fully in the course of the paper. The perturbation solutions have the added advantage of being asymptotically correct as they are derived in a rigorous manner using the method of matched asymptotic expansions. For purposes of clarity we consider the two types of drops separately using the same notation in each section rather than attaching suffixes to all variables.

Part 1. Sessile drops

2. Problem formulation

We consider figure 1, depicting a sessile liquid drop in equilibrium in an infinite fluid medium. For completeness we give a short derivation of the capillary equation. Here, r and z represent the polar coordinates of the drop surface, z representing distance below the apex or highest point. The drop shape is assumed axisymmetric. The hydrostatic pressure in the drop is given by $\rho gz + p^*$, where ρ is the density of the fluid and g the acceleration due to gravity. In this instance we have neglected the density of the surrounding fluid as for example would be reasonable in the case of a water drop in air. If the fluid density is not negligible the density ρ is taken to mean the liquid–fluid density differential. p^* is the pressure jump across the interface at $z = 0$ at the apex. At this point we diverge somewhat from traditional formulations of the problem where this excess pressure is given in terms of the unknown radius of curvature at the apex, the point being that the two radii of curvature are equal at this point. This is unnecessary and it proves simpler to determine p^* in the course of

the analysis. Along the interface the pressure is balanced by the capillary forces, giving rise to the following equation:

$$\gamma(1/R_1+1/R_2) = \rho gz+p^*, \tag{1}$$

where γ is the surface tension of the interface and R_1 and R_2 are the principle radii of curvature. The first of these is associated with the drop curvature when viewed in profile (in the (r,z)-plane of figure 1). The second term is curvature in a perpendicular plane containing the normal. Curvature can be positive or negative depending on which way the profile curves. The usual convention is applied here: radii of curvature are assigned positive values when the surface is concave when viewed from the liquid and negative otherwise. The relevant expressions for the two curvatures can be obtained from differential geometric results whereupon (1) becomes

$$\gamma\left\{\frac{\mathrm{d}^2z/\mathrm{d}r^2}{[1+(\mathrm{d}z/\mathrm{d}r)^2]^{\frac{3}{2}}}+\frac{\mathrm{d}z/\mathrm{d}r}{r[1+(\mathrm{d}z/\mathrm{d}r)^2]^{\frac{1}{2}}}\right\}-\rho gz = p^*. \tag{2}$$

As already pointed out, previous analyses have used (2) as starting point with p^* given in terms of the radius of curvature at the apex. We will not be using this equation as it stands but it will nevertheless turn out to be extremely important when we seek to rescale variables in different regions. Appealing again to differential geometry we can replace (2) with the following system:

$$\gamma\left\{\frac{\mathrm{d}\phi}{\mathrm{d}s}+\frac{\sin\phi}{r}\right\}-\rho gz = p^*, \tag{3a}$$

$$\frac{\mathrm{d}r}{\mathrm{d}s} = \cos\phi, \quad \frac{\mathrm{d}z}{\mathrm{d}s} = \sin\phi, \tag{3b, c}$$

where ϕ is the inclination at any point (r,z) and s is the arclength measured from the apex. A considerable advantage of the new system is that we no longer have problems with infinite slopes ($\mathrm{d}z/\mathrm{d}r$ in (2)) when the drop profile becomes vertical. Rienstra (1990) used (3) to obtain first-order solutions for sessile drops. Arclength can be eliminated from (3): this appears desirable but introduces its own complications as mentioned in §22. Arclength is eliminated from (3), as in O'Brien & van den Brule (1991), yielding the following system:

$$\frac{\mathrm{d}r}{\mathrm{d}\phi} = \frac{\gamma r\cos\phi}{-\gamma\sin\phi+\rho grz+p^*r}, \qquad \frac{\mathrm{d}z}{\mathrm{d}\phi} = \frac{\gamma r\sin\phi}{-\gamma\sin\phi+\rho grz+p^*r}. \tag{4a, b}$$

This system of ordinary differential equations will be the starting point for our analyses. We consider r and z to be functions of the parameter ϕ, the independent variable, which is the angle of inclination. In the pendant problem this allows the derivation of an explicit equation for the point of inflexion. The occurrence of a point of inflexion means that the inclination ϕ changes direction there so it is important that its location be known explicitly.

The natural lengthscale existing in the problem is the capillary length given by $a = (\gamma/\rho g)^{\frac{1}{2}}$. Equation (4) is non-dimensionalized as follows:

$$X = r/a; \quad Y = z/a; \quad P = p^*/\rho ga, \tag{5}$$

whereupon (4) reduces to

$$\frac{\mathrm{d}X}{\mathrm{d}\phi} = \frac{X\cos\phi}{XY+XP-\sin\phi}, \qquad \frac{\mathrm{d}Y}{\mathrm{d}\phi} = \frac{X\sin\phi}{XY+XP-\sin\phi}. \tag{6a, b}$$

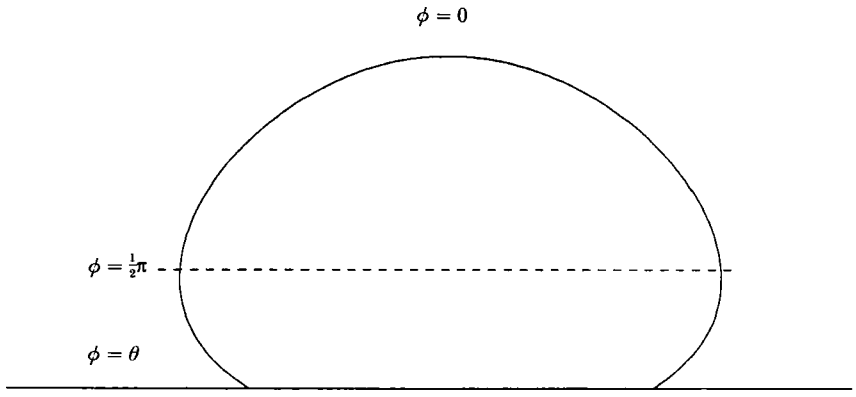

FIGURE 3. The equator of a sessile drop.

In the course of this paper, it is helpful to remember that X, Y, P are the fundamental dimensionless variables we choose to work with. This should clarify any confusion which arises due to the various scalings which are used in the course of the analysis.

3. Boundary conditions

A full solution of (6) requires one boundary condition for each first-order equation and a supplementary condition to solve for the unknown constant P. Referring to figure 1 we see that our choice of coordinate system fixes two conditions:

$$X = 0 \quad \text{and} \quad Y = 0 \quad \text{when} \quad \phi = 0. \tag{7}$$

The most obvious other condition would be given in terms of the contact angle at the base of the drop where it meets the horizontal substrate. However this is unnecessarily complicated: instead we formulate a condition at the point of maximum bulge of the drop. At this point (see figure 3) we have

$$X = R \quad \text{when} \quad \phi = \tfrac{1}{2}\pi, \tag{8}$$

where $R = L/a$ is the dimensionless drop radius at this point, L being the maximum radius of the drop in the physical variables. The important point here is that the shape of the drop is essentially determined by the values R and a. Once these are fixed the universal shape of the drop is determined: the contact angle merely determines the point at which the drop meets the substrate. Referring to figure 3 we can truncate the theoretical drop shape at the point where $\phi = \theta$. If $\theta = \frac{1}{2}\pi$ then the drop shape is given by that portion of figure 3 which exists above the dotted line. If $\theta < \frac{1}{2}\pi$ we truncate somewhere above the dotted line. Even though ϕ in reality never becomes equal to $\frac{1}{2}\pi$ in this case, condition (8) may still be used.

4. Scaling the equations

In order to carry out a successful parameter perturbation it is necessary to find the correct scalings for the different terms in (6) especially because of the existence of nonlinear terms. To this end consideration of (2) will prove extremely helpful. If a liquid drop becomes infinitely small, its shape is perfectly spherical and this will be the basis of a perturbation solution, the dimensionless radius being the small parameter. As this radius becomes very small the two curvature terms in (2) become very large and the body force term (ρgz) becomes negligible in the limit. The p^* must

also be of the same order as the curvature terms as these have the same sign and cannot balance one another. It is thus also necessary to scale the constant p^* (or more correctly the dimensionless P). The zero-order problem should thus represent a balance between curvature effects and p^*. Guided by these qualitative considerations we introduce the scalings which yield the correct balance at zero order. It is obvious that lengths should be scaled with R so we define scaled variables x, y, p:

$$X = Rx; \quad Y = Ry; \quad P = p/R. \tag{9}$$

The final scaled system is thus

$$\frac{\mathrm{d}x}{\mathrm{d}\phi} = \frac{x\cos\phi}{R^2xy + xp - \sin\phi}, \qquad \frac{\mathrm{d}y}{\mathrm{d}\phi} = \frac{x\sin\phi}{R^2xy + xp - \sin\phi}, \tag{10a, b}$$

with scaled boundary conditions

$$x = 0 \quad \text{and} \quad y = 0 \quad \text{when} \quad \phi = 0, \tag{11}$$

$$x = 1 \quad \text{when} \quad \phi = \tfrac{1}{2}\pi. \tag{12}$$

We are assuming that ϕ has $O(1)$ behaviour: this turns out to be correct except in the neighbourhood of π. We can now define what we mean by a small drop: we require that if L is the physical radius then $R \equiv L/a$ is a small number. Note that for pure water a is approximately 2.7 mm so for a water drop of radius 1 mm, R^2 is roughly 0.14. We now seek solutions of (10) in the following form:

$$x = x_0 + R^2x_1 + R^4x_2; \quad y = y_0 + R^2y_1 + R^4y_2; \quad p = p_0 + R^2p_1 + R^4p_2. \tag{13}$$

Note that because p is a constant, once it has been established that it is correctly scaled, this scaling remains valid everywhere. This is not necessarily the case for variables such as x and y whose order of magnitude can change in boundary layers.

5. Zero-order solutions

Substituting the series (13) into (10), we obtain to lowest order:

$$x_0p_0x_0' - x_0'\sin\phi = x_0\cos\phi, \qquad x_0p_0y_0' - y_0'\sin\phi = x_0\sin\phi, \tag{14a, b}$$

where differentiation with respect to ϕ is denoted by a prime. Applying the relevant boundary conditions:

$$x_0 = 0; \quad y_0 = 0 \quad \text{when} \quad \phi = 0, \tag{15}$$

$$x_0 = 1 \quad \text{when} \quad \phi = \tfrac{1}{2}\pi, \tag{16}$$

we obtain the following solutions:

$$x_0 = \sin\phi, \qquad y_0 = 1 - \cos\phi, \qquad p_0 = 2. \tag{17a–c}$$

As expected the zero-order solution gives a circular profile, describing a spherical drop.

6. First-order solutions

At this order we obtain

$$x_0y_0x_0' + x_0p_1x_0' + x_1p_0x_0' + x_0p_0x_1' - x_1'\sin\phi = x_1\cos\phi, \tag{18a}$$

$$x_0y_0y_0' + x_0p_1y_0' + x_1p_0y_0' + x_0p_0y_1' - y_1'\sin\phi = x_1\sin\phi. \tag{18b}$$

Applying the following boundary conditions:

$$x_1 = 0; \quad y_1 = 0 \quad \text{when} \quad \phi = 0, \tag{19a}$$

$$x_1 = 0 \quad \text{when} \quad \phi = \tfrac{1}{2}\pi, \tag{19b}$$

we obtain the solutions:

$$x_1 = \tfrac{1}{3}\cos^2\phi \tan\tfrac{1}{2}\phi, \tag{20a}$$

$$y_1 = \tfrac{1}{3}\cos\phi - \tfrac{1}{3}\cos^2\phi + \tfrac{2}{3}\ln(\cos\tfrac{1}{2}\phi), \tag{20b}$$

$$p_1 = -\tfrac{1}{3}. \tag{20c}$$

Solutions to second order are to be found in O'Brien & van den Brule (1991).

7. Solutions near $\phi = \pi$

A cursory glance at (20) indicates a singularity in the solutions at $\phi = \pi$ where both x_1 and y_1 blow up. This is of course physically unacceptable. The indications are that our scalings are incorrect near $\phi = \pi$ and it is found that a boundary layer occurs in this region and a stretched inner independent variable is necessary. The outer solutions, when ϕ is not near π, are then given by (17), (20). In addition the scale of the dependent variables x and y also changes in the boundary layer. Inspection indicates the following rescaled variables ξ, ζ, p, Φ to replace (9):

$$X = R^2\xi; \quad Y = 2R + R^3\zeta; \quad P = p/R; \quad \phi = \pi - R\Phi. \tag{21}$$

In fact only p is unchanged here. Strictly speaking we should more generally scale $Y = \alpha R + R^3\zeta$ but it is simpler to anticipate $\alpha = 2$ from physical considerations since at lowest order the drop is spherical, so near $\phi = \pi$, $Y = 2R + o(R)$. In addition we will only work to leading order so we will not attach suffixes: ξ and ζ are taken to be lowest order rather than writing ξ_0 and ζ_0. Extension to higher orders is straightforward but tedious. With these scalings, which indicate that the boundary layer is $O(R)$ in ϕ, (6a) now yields the following lowest-order boundary-layer equations for ξ and ζ:

$$p\xi\xi' - \Phi\xi' = \xi, \tag{22a}$$

$$-2\xi\zeta' + \Phi\zeta' = \xi\Phi, \tag{22b}$$

where the primes denote differentiation with respect to Φ. Bearing in mind that p cannot change order and is given to lowest order by (17c) we have $p = 2$ in (22). This can now be integrated, yielding

$$\Phi = \xi - C/\xi \quad \text{or} \quad \xi = \tfrac{1}{2}[\Phi \pm (\Phi^2 + 4C)^{\frac{1}{2}}], \tag{23a}$$

$$\zeta = -\tfrac{1}{4}\Phi(\Phi^2 + 4C)^{\frac{1}{2}} + C\ln[\Phi + (\Phi^2 + 4C)^{\frac{1}{2}}] - \tfrac{1}{4}\Phi^2 + N, \tag{23b}$$

where C and N are arbitrary integration constants to be obtained from matching with the outer solution. The positive root of (23a) is the relevant one. As solutions for the case when $\phi > \pi$ have no physical relevance to the problem of a drop resting on a *plane* horizontal surface (they actually represent a curling up of the drop profile on itself) we neglect them from now on. We note however that the situation with $\phi > \pi$ can occur, for example, in the case of a drop on top of a suitably shaped rod as discussed by Padday (1971). To describe this profile, one must continue the solution for $\phi \geqslant \pi$ and it should be borne in mind that (23) is only valid very close to $\phi = \pi$.

To continue the solution for $O(1)$ changes in ϕ it is necessary to rescale all variables once more in an analogous manner to that later adopted for the neck region of the pendant drop (§15).

8. Matching inner and outer solutions

To find the integration constants of (23) we match the outer solution obtained from (17a) and (20a) with inner solution (23a). We assume the existence of an intermediate overlap variable θ such that

$$\phi = \pi - \theta\eta(R); \quad \Phi = (\pi-\phi)/R = \theta\eta(R)/R; \quad O(1) \gg \eta(R) \gg R. \tag{24}$$

The outer solution, in fundamental dimensionless form (5), expanded for small η yields

$$R\theta\eta + 2R^3/3\theta\eta \tag{25}$$

while the inner solution gives

$$R\theta\eta + CR^3/\theta\eta \tag{26}$$

to the same order, provided $R \gg \eta^2$, which defines the overlap region. The solutions match identically to $O(R)$, justifying our $O(R)$ scaling of Y while matching to next order yields

$$C = \tfrac{2}{3}. \tag{27}$$

Proceeding with the Y matching using the same intermediate variable θ, the outer solution obtained from (17b) and (20b) yields

$$R(2-\tfrac{1}{2}\theta^2\eta^2) + \tfrac{1}{3}R^3(-2+\tfrac{1}{2}\theta^2\eta^2) + \tfrac{2}{3}R^3[\ln(\theta\eta) - \ln 2], \tag{28}$$

while the inner solution (23b) gives

$$2R - \tfrac{1}{2}R\theta^2\eta^2 - \tfrac{1}{2}R^3C + CR^3\ln(2\theta\eta/R) + NR^3. \tag{29}$$

At this point we run into a well-known phenomenon which often occurs in singular perturbation problems. (See for example Lagerstrom & Casten 1972.) As they stand (28) and (29) cannot be matched owing to the presence of $R^3\ln R$ terms in (29). Our analysis indicates that switchback terms are needed, i.e. that the scaling of ζ was not correct and there are some terms of between $O(R)$ and $O(R^3)$ which have been omitted. Formally we can remedy this by inserting an extra term $\zeta_{sw}R^3\ln R$ into the expansion for Y. On substituting this into (23b) we find that $\zeta_{sw} = D_{sw}$, an arbitrary constant, so we are free to add an extra term $D_{sw}R^3\ln R$ onto (29). In this way D_{sw} can be chosen so as to annihilate the $R^3\ln(R)$ terms and the matching can be successfully carried out. It yields the following results:

$$N = \tfrac{2}{3}(-2\ln 2 - \tfrac{1}{2}); \quad D_{sw} = \tfrac{2}{3}, \tag{30}$$

$$Y_{inner} = 2R + D_{sw}R^3\ln R^3 + R^3\zeta(\Phi), \tag{31}$$

where $\zeta(\Phi)$ is given by (23b) and Y_{inner} is in fundamental dimensionless form (5).

9. Comparison with previous results

Tables 1 and 2 compare the results of the present paper with the previous results of Chesters (1977) and the numerical results of Hartland & Hartley (1976) which may be taken to be exact. Table 1 includes solutions to second order which can be seen to compare favourably with the numerical solutions. Also included are the first-order results for comparison with Chesters'. Table 2 contains only first-order results. The

	x_c	y_c	x_c	y_c
	$(\beta = -0.0001)$ $(R = 0.00998)$		$(\beta = -0.01)$ $(R = 0.009983)$	
Chesters	0.999983	0.999960	0.998333	0.996023
Present (ϵ)	0.999993	0.999960	0.998342	0.996043
Present (ϵ^2)	0.999983	0.999960	0.998342	0.996054
Hartland	0.999983	0.999960	0.998342	0.996054
	$(\beta = -0.03162)$ $(R = 0.17689)$		$(\beta = -0.1)$ $(R = 0.3112)$	
Chesters	0.994730	0.987423	0.983333	0.960228
Present (ϵ)	0.994815	0.987622	0.984151	0.962127
Present (ϵ^2)	0.994815	0.987734	0.984151	0.963193
Hartland	0.994815	0.987730	0.984151	0.963129

TABLE 1. Comparison of sessile drop solutions of present paper with previous perturbation solution of Chesters and numerical solutions of Hartland & Hartley at $\phi = \frac{1}{2}\pi$, when the drop is vertical. β is Chesters' shape factor. The variables of the present paper are obtained by multiplying by $(-\beta)^{\frac{1}{3}}$.

	x	y	x	y
	$(\beta = -0.0001)$ $(R = 0.00998)$		$(\beta = -0.01)$ $(R = 0.099983)$	
Chesters	8.16497×10^{-3}	1.99957	8.16497×10^{-2}	1.97201
Present	8.16468×10^{-3}	1.99957	8.13791×10^{-2}	1.972139
Hartland	8.16415×10^{-3}	1.99957	8.08481×10^{-2}	1.97239
	$(\beta = -0.03162)$ $(R = 0.17689)$		$(\beta = -0.1)$ $(R = 0.3112)$	
Chesters	0.145196	1.92362	0.258199	1.79686
Present	0.1436878	1.924711	0.250079	1.80542
Hartland	0.140846	1.92656	0.236010	1.81742

TABLE 2. Comparison of boundary-layer sessile drop solutions to first order with previous perturbation solution of Chesters and numerical solutions of Hartland & Hartley at $\phi = \pi$, when the drop becomes horizontal.

solutions in the present paper are seen to be better in all cases. Nevertheless the solutions of Chesters stand up quite well given the *ad hoc* nature of his perturbation procedure. We note that β is the shape factor of Chesters. In order to obtain the small parameter $R = L/a$ of the present paper, we use the relationship $R = X_{\max}(-\beta)^{\frac{1}{2}}$ where $X_{\max}$ is obtained from the numerical (exact) results. Thus in table 1 the x-solutions are irrelevant and it is the y-solutions that should be examined. We also note that the x, y of tables 1 and 2 are given in terms of Chesters' variables for simplicity of comparison. To obtain the non-dimensional variables of (5) all values in tables 1 and 2 must be multiplied by $(-\beta)^{\frac{1}{3}}$.

By making use of the boundary-layer solutions we can explicitly write down the values of X and Y at the base of the drop where $\phi = \pi$. From (23*a*) and (23*b*), setting $\Phi = 0$ we obtain the following results:

$$X = (\tfrac{2}{3})^{\frac{1}{3}}R^2; \quad Y = 2R + \tfrac{1}{3}R^3(-1 - \ln 6) + \tfrac{2}{3}R^3 \ln R. \tag{32}$$

The first of these corresponds to Chesters' (56) while the second corrects his (57). Of

course his lengthscale is the radius of curvature at the top of the drop, but nevertheless we might expect the two results to be asymptotically equivalent in the limit. Comparison with numerical solution verifies that the present results are an improvement.

10. Composite solutions

It is, as usual, possible to derive an expression for a solution uniformly valid for $0 \leqslant \phi \leqslant \pi$, i.e. both inside and outside the boundary layer. Working to $O(R^3)$, the common part of X given in terms of the outer variable ϕ is

$$X_{\rm cp} = R(\pi-\phi)+2R^3/[3(\pi-\phi)] \tag{33}$$

and a composite solution is obtained by adding the outer and inner solutions (17*a*), (20*a*) and (23*a*) written in terms of the fundamental dimensionless variable X of (5) and subtracting (33). As (20*a*) has a singularity when $\phi = \pi$ which is obliterated by a similar singularity in (33), it may be desirable to write (20*a*) in a Taylor series near $\phi = \pi$ to avoid numerical difficulties by explicitly removing the singular terms.

Similarly the common part of Y to $O(R^3)$ is given by

$$Y_{\rm cp} = 2R-\tfrac{1}{2}R(\pi-\phi)^2-\tfrac{2}{3}R^3+\tfrac{2}{3}R^3\ln(\pi-\phi)-\tfrac{2}{3}R^3\ln 2. \tag{34}$$

A composite solution is given in terms of the fundamental variable Y using (17*b*), (20*b*) and (31). The inner and outer solutions are summed and the common part (34) is subtracted. Similar to the X case, numerical problems may be avoided by use of Taylor series near $\phi = \pi$.

Part 2. Pendant drops

11. Problem formulation

There are many similarities between the sessile and pendant drop problems which can be exploited. One basic difference is illustrated by figure 2 where a different choice of coordinate system illustrates that gravity forces act, in effect, in the opposite direction to the sessile case. The basic equation is still (1), but in this instance the sign of the ρgz-term changes. Carrying this sign change through the previous analysis, we obtain the following modified form of (6) in terms of the dimensionless variables (5):

$$\frac{{\rm d}X}{{\rm d}\phi} = \frac{X\cos\phi}{-XY+XP-\sin\phi}, \quad \frac{{\rm d}Y}{{\rm d}\phi} = \frac{X\sin\phi}{-XY+XP-\sin\phi}. \tag{35a, b}$$

The boundary conditions (7) and (8) remain identical.

12. Solution strategy

Before proceeding any further with the solutions, it is helpful to consider an overall strategy as suggested by the physics of the problem. An examination of figure 2 indicates that the bottom part of the drop will again resemble a circle as in the sessile case. We can expect the higher-order corrections to tend to elongate the drop rather than flattening it as in the sessile case. It is thus physically reasonable, and analysis verifies this, to expect no more than changes in sign in the lower solution, henceforth referred to as the outer solution, when compared to the equivalent part of the sessile

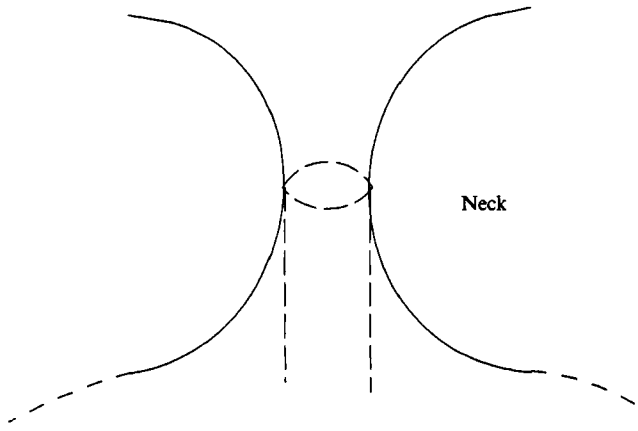

FIGURE 4. Schematic drawing of drop neck.

drop. However, as the inclination passes monotonically from 0 through $\frac{1}{2}\pi$ and again approaches π, a qualitative change occurs in the drop shape which has no analogue in the sessile case. A point of inflexion occurs and the inclination ϕ changes direction, attaining some maximum value ϕ_i and then decreasing monotonically towards a minimum ϕ_m at the extreme top of the drop. If the contact angle is not equal to this minimum, the drop shape can be truncated at the point where the inclination does equal the contact angle.

If we momentarily ignore the behaviour of the solutions near the inflexion point, we may enquire what happens in the neck region. Hereafter we will refer to solutions in this region as the neck solutions. It is clear that the drop shape in the neck does not even vaguely resemble a sphere: this indicates that our problem will need rescaling in this region. The key to the neck region is illustrated in figure 4. This illustrates that the drop shape in the neck region is in fact of the same form as the meniscus near a small cylinder with contact angle equal to $\frac{1}{2}\pi$. In this region, if δ is a scale for the cylinder radius, then $\delta \ll R$ and scaling x and y with δ as in James (1974) yields a lowest-order balance between the curvature terms of (2) or (3). The precise size of δ is initially unknown but can be derived from matching with the interior-layer solution.

This leads naturally to the problem of the matching. The neck solution would appear to be valid from the point of inflexion to the uppermost point of the drop, thus as ϕ *decreases* from ϕ_i to its minimum value. The outer solution should be valid from the bottom of the drop to near the point of inflexion, thus as ϕ *increases* from zero to ϕ_i. In addition, the outer solution (like the sessile drop case) displays a singularity at $\phi = \pi$ and it is not immediately obvious if the solutions at the point of inflexion (which is asymptotically near $\phi = \pi$) are valid. Not too surprisingly, it turns out that the outer and neck solutions cannot be matched. Completely analogous to the sessile case, there exists a transition or interior boundary layer in ϕ of $O(R)$ but in this instance it is centred about the point of inflexion rather than $\phi = \pi$. The outer solution can be matched to this on one side and the neck solution on the other side.

A final complication arises at the top of the neck region. As ϕ tends to its minimum, the neck solution becomes singular and it is necessary to insert another

boundary layer near $\phi = 0$. Mathematically, this region is very similar to the interior-layer region about the point of inflexion, the analysis being virtually identical. Analogous to the point of inflexion, there exists a value of ϕ below which no solutions exist. This limiting value can be interpreted as a second point of inflexion.

In summary the solution consists of four regions: an outer nearly circular region, an inner interior-layer region near $\phi = \pi$, a neck region resembling the meniscus near a small cylinder, and another boundary layer region at the uppermost extremity of the drop.

13. Outer solution

In this region, the scalings (9) are relevant and the scaled system is

$$\frac{\mathrm{d}x}{\mathrm{d}\phi} = \frac{x\cos\phi}{-R^2xy + xp - \sin\phi}, \quad \frac{\mathrm{d}y}{\mathrm{d}\phi} = \frac{x\sin\phi}{-R^2xy + xp - \sin\phi}. \tag{36a, b}$$

The boundary conditions (11) and (12) are still valid and we again seek solutions of the form (13). The zero-order equations and solutions turn out to be identical as given in §5. Equations (17) are thus valid.

The first-order solutions are equivalent except for a change in sign. The equations are:

$$-x_0y_0x_0' + x_0p_1x_0' + x_1p_0x_0' + x_0p_0x_1' - x_1'\sin\phi = x_1\cos\phi, \tag{37a}$$

$$-x_0y_0y_0' + x_0p_1y_0' + x_1p_0y_0' + x_0p_0y_1' - y_1'\sin\phi = x_1\sin\phi, \tag{37b}$$

with solutions

$$x_1 = -\tfrac{1}{3}\cos^2\phi\tan(\tfrac{1}{2}\phi), \tag{38a}$$

$$y_1 = -\tfrac{1}{3}\cos\phi + \tfrac{1}{3}\cos^2\phi - \tfrac{2}{3}\ln[\cos(\tfrac{1}{2}\phi)], \tag{38b}$$

$$p_1 = \tfrac{1}{3}. \tag{38c}$$

Similarly the second-order solutions are given by

$$\begin{aligned} -x_2\sin\phi = {} & \tfrac{1}{12}\cos\phi + \tfrac{1}{36}\cos 3\phi - \tfrac{1}{8}\sin^4\phi + \tfrac{1}{24}\cos^4\phi \\ & - (\tfrac{1}{8} + \tfrac{1}{12}\ln 2)\cos 2\phi - \tfrac{1}{2}p_2\sin^2\phi \\ & + \tfrac{1}{12}\{\ln(2\cos^2[\tfrac{1}{2}\phi])[\cos 2\phi - 1] + 2\cos\phi - \cos^2\phi\} \\ & - \tfrac{2}{3}\{\sin^2[\tfrac{1}{2}\phi]\sin\phi\cos^2\phi\tan[\tfrac{1}{2}\phi] + \tfrac{1}{6}\cos^3\phi - \tfrac{1}{8}\cos^4\phi\} \\ & - \tfrac{1}{2}p_0x_1^2 - p_1x_0x_1 - \tfrac{1}{12} + \tfrac{1}{12}\ln 2, \end{aligned} \tag{39a}$$

$$\begin{aligned} -y_2 = {} & -\tfrac{1}{6}\ln 2 + \cos\phi(\tfrac{1}{6}\ln 2 + \tfrac{23}{18}) - \tfrac{5}{9}\cos^2\phi + \tfrac{2}{9}\cos^3\phi \\ & - 3\cos\phi/\sin^2\phi\{-\tfrac{1}{27}\cos^4\phi + \tfrac{1}{9}\cos^3\phi - \tfrac{8}{27}\cos^2\phi - \tfrac{2}{9}\cos\phi + \tfrac{4}{9}) \\ & + \ln\{\cos[\tfrac{1}{2}\phi]\}(-\tfrac{1}{3}\cos\phi - \tfrac{2}{9}) - y_0y_1 + \tfrac{1}{3}y_1, \end{aligned} \tag{39b}$$

$$-p_2 = \tfrac{1}{3}\ln 2 - \tfrac{1}{6}. \tag{39c}$$

14. Interior-layer solution

As in the sessile drop case we again stretch the independent variable ϕ using the scalings (21). The lowest-order boundary-layer equation for ξ is again (22a) yielding a solution similar to (23a) but with a different integration constant:

$$\Phi = \xi - D/\xi \quad \text{or} \quad \xi = \tfrac{1}{2}[\Phi \pm (\Phi^2 + 4D)^{\frac{1}{2}}]. \tag{40a, b}$$

The constant D is found by matching with the outer solution. The analysis of the matching is similar to the sessile case and yields

$$D = -\tfrac{2}{3}. \tag{41}$$

This is reminiscent of (27) but in fact the negative sign is extremely significant. Equation (40) has no solutions for $\Phi = 0$ ($\phi = \pi$), which we might have expected as the drop never becomes horizontal again. In fact (40) has no solutions for $\Phi < (\frac{8}{3})^{\frac{1}{2}}$ and in fact this defines our inflexion point to $O(R)$, which occurs when $\mathrm{d}\Phi/\mathrm{d}\xi = 0$ and is explicitly given by

$$\Phi = (\tfrac{8}{3})^{\frac{1}{2}} \quad \text{or} \quad \phi = \pi - R(\tfrac{8}{3})^{\frac{1}{2}}. \tag{42}$$

This relationship can be easily verified by a consideration of the numerical solutions of Hartland & Hartley. Furthermore both branches of (40) are relevant: the positive root is valid before the point of inflexion is reached and ϕ is still increasing, after which the solution switches to the negative root and ϕ decreases towards zero.

The boundary-layer equation for ζ turns out to be identical to (22*b*) yielding the following *lower* interior-layer solution before the point of inflexion:

$$\zeta = -\tfrac{1}{4}\Phi(\Phi^2+4D)^{\frac{1}{2}} + D\ln[\Phi+(\Phi^2+4D)^{\frac{1}{2}}] - \tfrac{1}{4}\Phi^2 + M, \tag{43a}$$

where we have also used the positive root of (40). The constant M will be obtained from the matching while D is given by (41).

Beyond the point of inflexion, the negative root of (40) is valid. Substituting this into the boundary-layer equation (22*b*) we obtain the following *upper* interior-layer expression for ζ *beyond* the point of inflexion:

$$\zeta = \tfrac{1}{4}\Phi(\Phi^2+4D)^{\frac{1}{2}} - D\ln[\Phi+(\Phi^2+4D)^{\frac{1}{2}}] - \tfrac{1}{4}\Phi^2 + Q', \tag{43b}$$

in which Q' has yet to be determined. In addition we will demand that (43*a*) and (43*b*) are continuous across the point of inflexion as an extra condition. For this reason it is convenient to rewrite (43*b*) as follows:

$$\zeta = \tfrac{1}{4}\Phi(\Phi^2+4D)^{\frac{1}{2}} + D\ln[\Phi+(\Phi^2+4D)^{\frac{1}{2}}] - \tfrac{1}{4}\Phi^2 + Q, \tag{43c}$$

as continuity of (43*a*) and (43*c*) merely requires that $M = Q$. Before proceeding with the matching, we consider the neck region.

15. The neck solutions

As already elucidated, the scaling for the neck region requires a dominant balance between the curvature terms of (2). We introduce the following new scalings obtained by inspection:

$$X = \delta(R)\,u; \quad Y = 2R + \delta(R)\,v, \tag{44}$$

where $\delta(R)$ is an unknown function. We do know that $\delta(R) \ll R$ as otherwise (35) will not yield the correct balance. The easiest way to see this is by a consideration of the dimensionless form of (2). We expect that ϕ is $O(1)$ and leave it unscaled. We will again only work to lowest order and will not use suffices on the u and v to demonstrate the order. The lowest-order equations are:

$$\frac{\mathrm{d}u}{\mathrm{d}\phi} = -u\cot\phi, \qquad \frac{\mathrm{d}v}{\mathrm{d}\phi} = -u, \tag{45a, b}$$

with the solutions

$$u = A \operatorname{cosec} \phi, \qquad v = -A \ln [\tan (\tfrac{1}{2}\phi)] + B. \tag{46a, b}$$

These are in fact the parametric equations of the meniscus near a small cylinder. The constants A and B, and the gauge function $\delta(R)$ will be found during the matching with the upper interior-layer solution.

16. The top boundary layer

As the inclination ϕ approaches ϕ_m near the top of the neck region (46) indicates that the solutions may become singular. This again indicates the occurrence of a boundary layer, which again turns out to be $O(R)$ in ϕ. The analysis is similar to that at the bottom of the neck region; we refer to this new boundary layer as the top layer. The scalings (21) are valid again except that ϕ is approaching 0 in this case so the stretched inner variable is defined by

$$\phi = R\Phi. \tag{47}$$

The boundary-layer equation for ξ is now

$$2\xi\xi' - \Phi\xi' = \xi, \tag{48}$$

with solution: $$\Phi = \xi - E/\xi \quad \text{or} \quad \xi = \tfrac{1}{2}[\Phi - (\Phi^2 + 4E)^{\frac{1}{2}}], \tag{49}$$

where E will be determined by matching with the neck solution. The negative root is used in (49) because it turns out to be the one which matches with the neck region.

Similarly the boundary-layer equation for ζ is

$$2\xi\zeta' - \Phi\zeta' = \xi\Phi, \tag{50}$$

with solution $$\zeta = -\tfrac{1}{4}\Phi(\Phi^2 + 4E)^{\frac{1}{2}} + E \ln [\Phi + (\Phi^2 + 4E)^{\frac{1}{2}}] + \tfrac{1}{4}\Phi^2 + S, \tag{51}$$

where the integration constants will be determined in the matching.

17. Matching of outer solution and lower interior-layer solution

The X matching has already been completed. The Y (or ζ) matching involves (43a) and the outer solution obtained from (17b) and (38b). The matching is similar to the case of the sessile drop with the occurrence of $R^3 \ln R$ terms necessitating the need to again include switchback terms as in the sessile case. Without repeating the details, we obtain the following for the lower solution:

$$\zeta = -\tfrac{1}{4}\Phi(\Phi^2 - \tfrac{8}{3})^{\frac{1}{2}} - \tfrac{2}{3} \ln [\Phi + (\Phi^2 - \tfrac{8}{3})^{\frac{1}{2}}] - \tfrac{1}{4}\Phi^2 + \tfrac{1}{3} + \tfrac{4}{3} \ln 2 - \tfrac{2}{3} \ln R, \tag{52}$$

so in (43a) $M = \frac{1}{3} + \frac{4}{3} \ln 2 - \frac{2}{3} \ln R$, the latter term being a switchback. At this point the solution is fully determined up to the point of inflexion.

18. Matching of upper interior-layer solution and neck solution

Beginning with the X (or ξ, u) matching, the solutions to be matched are (40b) and (46a). We again introduce an intermediate variable θ and a gauge function $\eta(R)$ such that $1 \gg \eta \gg R$. Working in terms of the fundamental variable X, and setting $\Phi = \theta\eta/R$ (40b) yields the following leading-order expansion as $\eta \to 0$:

$$2R^3/3\theta\eta$$

while (46*a*) with $\phi = \pi - \theta\eta$ yields

$$A\delta/\theta\eta$$

and matching yields both the constant A and the gauge function δ:

$$A = \tfrac{2}{3}; \quad \delta(r) = R^3.$$

This indicates that the radius of the imaginary cylinder of figure 4, i.e. the minimum width of the neck is $\frac{2}{3}R^3$.

Continuing with the Y matching, the relevant equations are (43*c*) and (46*b*). Introducing the intermediate variable θ again and setting $\phi = \pi - \theta\eta$, (46*b*) gives the following limiting expansion in terms of the fundamental variable Y:

$$2R - \tfrac{2}{3}R^3 \ln 2 + \tfrac{2}{3}R^3 \ln(\theta\eta) + BR^3, \tag{53}$$

while (43*c*), with $\Phi = \theta\eta/R$ yields

$$2R - \tfrac{1}{3}R^3 + \tfrac{2}{3}R^3 \ln(\theta\eta) + \tfrac{2}{3}R^3 \ln\tfrac{4}{3} - \tfrac{2}{3}R^3 \ln R + QR^3. \tag{54}$$

Equations (53) and (54) show two apparent sources of difficulty. In the first place they both contain unknown constants B and Q and secondly we note again the occurrence of $R^3 \ln R$-terms in (54) which do not correspond to any term in (53). The first of these difficulties is resolved by the fact that the lower and upper solutions (43*a*) and (43*c*) should be continuous at the point of inflexion so we have

$$Q = M = \tfrac{1}{3} + \tfrac{4}{3}\ln 2 - \tfrac{2}{3}\ln R \tag{55}$$

adding switchbacks as required. In this way (43*b*), the upper interior-layer solution becomes

$$\zeta = \tfrac{1}{4}\Phi(\Phi^2 + 4D)^{\frac{1}{2}} + D\ln[\Phi - (\Phi^2 + 4D)^{\frac{1}{2}}] - \tfrac{1}{4}\Phi^2 + \tfrac{1}{3} + \tfrac{4}{3}\ln 2 - \tfrac{2}{3}\ln R. \tag{56}$$

The constant B can now be determined from the matching of (53) and the modified form of (54) which is

$$2R - \tfrac{1}{3}R^3 + \tfrac{2}{3}R^3 \ln(\theta\eta) - \tfrac{2}{3}R^3 \ln\tfrac{4}{3} - \tfrac{2}{3}R^3 \ln R + QR^3,$$

Q being given by (55). Clearly switchback terms $-\frac{4}{3}\ln R$ are also needed in (53), whereupon matching gives the relationship

$$B = \tfrac{2}{3}\ln 6. \tag{57}$$

The solution for the neck region in terms of the fundamental variable Y now reads

$$T = 2R - \tfrac{2}{3}R^3 \ln[\tan(\tfrac{1}{2}\phi)] + BR^3 - \tfrac{4}{3}R^3 \ln R, \tag{58}$$

where B is given in (57).

19. Matching of neck and top boundary layer

Without repeating the details, matching (46*a*) and (49) using an intermediate variable $\theta\eta(R)$ gives the result: $E = -\frac{2}{3}$. Similarly the expression for ζ in (51) becomes

$$\zeta = -\tfrac{1}{4}\Phi(\Phi^2 - \tfrac{8}{3})^{\frac{1}{2}} - \tfrac{2}{3}\ln[\Phi + (\Phi^2 - \tfrac{8}{3})^{\frac{1}{2}}] + \tfrac{1}{4}\Phi^2 + \tfrac{2}{3}\ln 24 - \tfrac{1}{3} - 2\ln R, \tag{59}$$

where switchback terms have been added as required. Equation (49) now shows Φ to have a minimum value of $(\frac{8}{3})^{\frac{1}{2}}$, i.e. $\phi_m = (\frac{8}{3})^{\frac{1}{2}}R$. At this point $\mathrm{d}\Phi/\mathrm{d}\xi$ is again zero, another inflexion point occurs and so ϕ again changes direction and begins to increase once more. The shape of the top boundary layer is a mirror image of the interior layer

and it is possible to continue the solution upwards to obtain a sequence of drops, each one connected by a neck to the preceding one. The analysis in this case proceeds much as before.

20. Composite solutions for the pendant drop

In this instance it is not possible to derive one composite solution for the whole problem. Two are required: one of these is valid below the point of inflexion and the other above it. In the matching of the outer solution and the lower interior-layer solution we obtain the following common part for X:

$$X_{\text{lcp}} = R(\pi-\phi)-2R^3/[3(\pi-\phi)], \tag{60}$$

so to $O(R^3)$ the lower composite X-solution is given by summing the outer solution (17a), (38a) and the lower interior-layer solution (40a) and subtracting (60). Similarly the common part of Y in the lower region is

$$Y_{\text{lcp}} = 2R-\tfrac{1}{2}R(\pi-\phi)^2+\tfrac{2}{3}R^3-\tfrac{2}{3}R^3\ln(\pi-\phi)+\tfrac{2}{3}R^3\ln 2 \tag{61}$$

and the relevant solutions are (17b), (38a) and (43a).

In the upper region the common part of X is

$$X_{\text{ucp}} = 2R^3/[3(\pi-\phi)], \tag{62}$$

the relevant constituent solutions being the upper interior-layer solution (40b) and the neck solution (46a). The common part of Y in this region is

$$Y_{\text{ucp}} = -\tfrac{2}{3}R^3\ln 2+\tfrac{2}{3}R^3\ln\{\pi-\phi\}+R^3(\tfrac{2}{3}\ln 6-\tfrac{4}{3}\ln R)+2R, \tag{63}$$

the constituent solutions being (56) and (58).

For the neck and top-layer solutions we obtain the following common parts in terms of the fundamental variables:

$$X_{\text{tcp}} = 2R^3/(3\phi), \tag{64}$$

$$Y_{\text{tcp}} = -\tfrac{2}{3}R^3\ln\phi+\tfrac{2}{3}R^3\ln 12-\tfrac{4}{3}R^3\ln R+2R. \tag{65}$$

A complete composite solution for the portion of the drop extending from the point of inflexion to the top is obtained by adding the upper interior-layer, neck and top boundary-layer solutions and subtracting the common parts (64) and (65).

21. Comparison with previous results

Tables 3 and 4 compare the results of the analysis of this paper with previous results of Chesters (1977) and the 'exact' numerical results of Hartland & Hartley (1976). The higher-order solutions for the outer problem are included. The results of the present paper are seen to be better in all cases when compared to Chesters' solutions. The area where the solutions are worst is the neck, in particular the X-values – although this could partly be expected as X is $O(R^2)$ in this region while Y is $O(R^3)$. Extension to higher order seems possible though tedious but it is unclear how to obtain better estimates of the point of inflexion though the arclength formulation (3) may be suitable as discussed in §22. It is interesting to include some other asymptotic results. At the point of inflexion we have the following expressions:

$$X = (\tfrac{2}{3})^{\frac{1}{3}}R^2, \tag{66}$$

$$Y = 2R+R^3(-\tfrac{1}{3}-\tfrac{2}{3}\ln R+\tfrac{1}{3}\ln 6). \tag{67}$$

	x_c	y_c	x_c	y_c
	($\beta = -0.0001$) ($R = 0.00998$)		($\beta = -0.01$) ($R = 0.099983$)	
Chesters	1.00002	1.00004	1.00167	1.00398
Present (ϵ)	1.00002	1.00004	1.00168	1.00400
Present (ϵ^2)	1.00002	1.00004	1.00168	1.00401
Hartland	1.00002	1.00004	1.00168	1.00401
	($\beta = -0.03162$) ($R = 0.17689$)		($\beta = -0.1$) ($R = 0.3112$)	
Chesters	1.00527	1.01258	1.01592	1.03798
Present (ϵ)	1.00536	1.01278	1.01668	1.03986
Present (ϵ^2)	1.00536	1.01298	1.01668	1.04177
Hartland	1.00536	1.01291	1.01668	1.04120

TABLE 3. Comparison of 'outer solutions' for pendant drop with previous perturbation solution of Chesters and numerical solutions of Hartland & Hartley, at $\phi = \frac{1}{2}\pi$, when the drop is vertical. β is Chesters' shape factor. To convert to the variables of the current paper all values should be multiplied by $\beta^{\frac{1}{3}}$.

(*a*) $\phi = \phi_1$	x_c	y_c	x_c	y_c
	($\beta = 10^{-4}$)		($\beta = 10^{-2}$)	
Chesters	8.16497×10^{-3}	2.00037	8.16497×10^{-2}	2.02132
Present	8.16530×10^{-3}	2.00037	8.19242×10^{-2}	2.02142
Hartland	8.16578×10^{-3}	2.00037	8.24789×10^{-2}	2.02160
	($\beta = 0.03162$)		($\beta = 0.09550$)	
Chesters	0.145196	2.0552	0.252322	2.13180
Present	0.14680	2.05607	0.26081	2.13731
Hartland	0.15000	2.05732	0.28000	2.14385
(*b*) $\phi = \frac{1}{2}\pi$	x_c	y_c	x_c	y_c
	($\beta = 10^{-4}$)		($\beta = 10^{-3}$)	
Chesters	6.66667×10^{-5}	2.000777	6.66667×10^{-3}	2.04598
Present	6.6671×10^{-5}	2.00077	6.7003×10^{-3}	2.0462
Hartland	6.66778×10^{-5}	2.00077	6.7796×10^{-3}	2.0466
	($\beta = 0.03162$)		($\beta = 0.09550$)	
Chesters	2.10819×10^{-2}	2.12113	6.3666×10^{-2}	2.29544
Present	2.14207×10^{-2}	2.12286	6.6905×10^{-2}	2.30816
Hartland	2.22551×10^{-2}	2.12691	7.5705×10^{-2}	2.33781

TABLE 4. Comparison of pendant drop results (*a*) at the point of inflexion, $\phi = \phi_1$, and (*b*) in the neck region where the drop becomes vertical, $\phi = \frac{1}{2}\pi$. To obtain the variables of the present paper all values are multiplied by $\beta^{\frac{1}{3}}$.

The first of these compares with Chesters' equation (34) while the second corrects his equation (47). In the neck region where the drop becomes vertical, we have

$$X = \tfrac{2}{3}R^3, \tag{68}$$

$$Y = 2R + R^3(\tfrac{2}{3}\ln 6 - \tfrac{4}{3}\ln R). \tag{69}$$

	Present		Hartland & Hartley	
ϕ	X	Y	X	Y
10	1.736539×10^{-2}	1.520084×10^{-3}	1.73655×10^{-2}	1.51931×10^{-3}
30	5.001643×10^{-2}	1.340531×10^{-2}	5.00164×10^{-2}	1.34042×10^{-2}
50	7.666821×10^{-2}	3.577155×10^{-2}	7.66680×10^{-2}	3.57700×10^{-2}
70	9.409905×10^{-2}	6.596862×10^{-2}	9.40991×10^{-2}	6.59655×10^{-2}
90	1.001668×10^{-1}	1.004030×10^{-1}	1.00168×10^{-1}	1.00401×10^{-1}
110	9.406868×10^{-2}	1.349582×10^{-1}	9.40700×10^{-2}	1.34598×10^{-1}
130	7.642943×10^{-2}	1.654946×10^{-1}	7.64298×10^{-2}	1.65499×10^{-1}
150	4.911343×10^{-2}	1.883886×10^{-1}	4.91083×10^{-2}	1.88400×10^{-1}
170	1.182661×10^{-2}	2.015297×10^{-1}	1.17548×10^{-2}	2.01566×10^{-1}
170.602	(numerical)			
170.627	8.210917×10^{-3}	2.021452×10^{-1}	8.24789×10^{-3}	2.02160×10^{-1}
170	5.712326×10^{-3}	2.025626×10^{-1}	5.78718×10^{-3}	2.02575×10^{-1}
150	1.373161×10^{-3}	2.037129×10^{-1}	1.38480×10^{-3}	2.03749×10^{-1}
130	8.819150×10^{-4}	2.041011×10^{-1}	8.89304×10^{-4}	2.04143×10^{-1}
110	7.161492×10^{-4}	2.043784×10^{-1}	7.22129×10^{-4}	2.04424×10^{-1}
90	6.723577×10^{-4}	2.046199×10^{-1}	6.77968×10^{-4}	2.04669×10^{-1}
70	7.161492×10^{-4}	2.048614×10^{-1}	7.22129×10^{-4}	2.04915×10^{-1}
50	8.819150×10^{-4}	2.051387×10^{-1}	8.89303×10^{-4}	2.05196×10^{-1}
30	1.373161×10^{-3}	2.055269×10^{-1}	1.38480×10^{-3}	2.05590×10^{-1}
10	5.712326×10^{-3}	2.066772×10^{-1}	5.78624×10^{-3}	2.06764×10^{-1}
9.39698	(numerical)			
9.372	8.21091×10^{-3}	2.07095×10^{-1}	8.24915×10^{-3}	2.07179×10^{-1}

TABLE 5. Comparison of pendant drop numerical results of Hartland & Hartley with composite solutions of present paper. $R = 0.100168$, Hartland's shape factor $B = 10^{-1}$. X and Y are the dimensionless fundamental variables of this paper.

Again the second of these corrects Chesters' result. At the topmost extremity of the drop X is again given by (66) while Y is given by

$$Y = 2R + R^3(\ln 6 + \tfrac{1}{3} - 2\ln R). \tag{70}$$

The value of ϕ at this point is given by $\phi = \phi_m = (\frac{8}{3})^{\frac{1}{2}}R$.

Finally table 5 compares a full set of solutions, this time in terms of the variables (5), with numerical solutions of Hartland & Hartley. The composite solutions of this paper are used, which are slightly less accurate than the relevant constituent solutions. Also included are a comparison of the numerical and asymptotic expressions for ϕ_l and ϕ_m.

22. A comment on the point of inflexion

The alternative formulations of the problem, (2) and (3), may be better frameworks for describing solutions near the point of inflexion in that it is no longer necessary to determine this point explicitly. For example, if we non-dimensionalize (3) using (5) supplemented by a dimensionless arclength $s = t/a$ and then scale using (21) supplemented by $t = 2\pi R + R^2\tau$, τ being scaled arclength, we obtain the following expression for Y as a function of ξ valid through the inflexion point:

$$Y = 2R + R^3(-\tfrac{1}{2}\xi^2 - \tfrac{2}{3}\ln\xi + \tfrac{2}{3}\ln 2 - \tfrac{2}{3}\ln R).$$

This result can also be obtained by eliminating Φ from the interior-layer equations.

23. Conclusions

We have revisited the problem of obtaining closed-form solutions for small sessile and pendant drops. Both problems showed singular or non-uniform behaviour, the method of matched asymptotic expansions being used in the course of the analysis. The sessile solutions are completely satisfactory when compared to numerical results, extension to higher-order approximations being straightforward. The pendant drop solutions are rather more complicated and interesting, a number of different scalings and boundary layers being required for an understanding of the solutions. This paper is not an exhaustive examination of the two problems, but it does explain the mathematical structure of the solutions. These might be extended to higher orders though the algebra quickly becomes extremely tedious.

The author would like to thank Dr A. B. Tayler and Dr A. C. Fowler for advice and suggestions during the preparation of this paper. I would further like to thank Professor D. H. Peregrine for his careful reading of the manuscript and several suggestions for improving it.

REFERENCES

BASHFORTH, F. & ADAMS, J. C. 1883 *The Theories of Capillary Action.* Cambridge University Press.

CHESTERS, A. K. 1977 An analytical solution for the profile and volume of a small drop or bubble symmetrical about a vertical axis. *J. Fluid Mech.* **81**, 609–624.

HARTLAND, S. & HARTLEY, R. W. 1976 *Axisymmetric Fluid Interfaces.* Elsevier.

JAMES, D. F. 1974 The meniscus on the outside of a small circular cylinder. *J. Fluid Mech.* **63**, 659–664.

KUIKEN, H. K. 1991 A single-parameter method for the determination of surface tension and contact angle. *Colloids and Surfaces* (submitted).

LAGERSTROM, P. A. & CASTEN, R. G. 1972 Basic concepts underlying singular perturbation techniques. *SIAM Rev.* **14**, 63–120.

O'BRIEN, S. B. G. & BRULE, B. H. A. A. VAN DEN 1991 *J. Chem. Soc., Faraday Trans. I* (submitted).

PADDAY, J. F. 1971 The profiles of axially symmetric menisci. *Phil. Trans. R. Soc. Lond.* A **269**, 265–293.

PADDAY, J. F. & PITT, A. R. 1972 Surface and interfacial tensions from the profile of a sessile drop. *Proc. R. Soc. Lond.* A **329**, 421–431.

RIENSTRA, S. W. 1990 The shape of a sessile drop for small and large surface tension. *J. Engng Maths* **24**, 193–202.

SHANAHAN, M. E. R. 1982 An approximate theory describing the profile of a sessile drop. *J. Chem. Soc., Faraday Trans. I* **78**, 2701–2710.